Int J Adv Manuf Technol (2014) 70:2249–2261
DOI 10.1007/s00170-013-5440-9

ORIGINAL ARTICLE

Tool orientation optimization and location determination for four-axis plunge milling of open blisks

Yongshou Liang · Dinghua Zhang · Zezhong C. Chen · Junxue Ren · Xiangyu Li

Received: 13 July 2013 / Accepted: 15 October 2013 / Published online: 17 November 2013

Abstract Plunge milling has been widely adopted in the manufacturing industry to rough machine open blisks, and its objective is to remove stock material with high efficiency and machining stability. A current technique challenge is to calculate the tool orientation and locations (called plunger paths) in four-axis rough plunging of open blisks, so that the residual raw material left on the blades after roughing is close to the specified value. To address this challenge, a novel approach is proposed to optimize tool orientation and determine tool locations for four-axis plunge milling of open blisks. First, tool locations are determined with two principles without interfering the blades and hub. Second, tool orientation is optimized according to a new evaluation criterion. Then, considering the impact of previous tool paths, an in-process model of a blisk is used to calculate residual material. Finally, an experiment is conducted to verify this new approach. This approach can promote four-axis plunge milling in the open blisk manufacturing.

Y. Liang (✉) · D. Zhang · J. Ren · X. Li
School of Mechanical Engineering, Northwestern Polytechnical University, Xi'an 710072, China
e-mail: liangys363@gmail.com

D. Zhang
e-mail: dhzhang@nwpu.edu.cn

J. Ren
e-mail: rjx1968@nwpu.edu.cn

X. Li
e-mail: 1lixiangyu1@mail.nwpu.edu.cn

Z.C. Chen
Department of Mechanical and Industrial Engineering, Concordia University, Quebec H3G 1M8, Montreal, Canada
e-mail: zcchen@encs.concordia.ca

Keywords Four-axis plunge milling · CNC programming for plunging · Open blisk machining · Tool path planning

1 Introduction

Blisks, also known as bladed disks or integrally bladed rotors (IBRs), are rotating portions of a fan or compressor stage of a jet engine. Blisks reduce the engine's weight, part count, and aerodynamic losses by manufacturing rotor disks and blades together, instead of traditional usage of the dovetail attachment [1]. Open blisks are usually machined in four-axis machine tools to reduce equipment and machining cost, especially for small enterprises. When cutting an open blisk, roughing process removes about 90 % of stock material and forms irregular machined surfaces on the blade for semi-finishing and finishing processes. It is of great importance to plan roughing process efficiently and appropriately to reduce cycle times and improve cutting conditions for the following processes.

To avoid collision and interference, slight cutting tools are adopted to cut the deep and narrow channels of open blisks. However, slight cutting tools with low rigidity cannot bear high radial cutting force when machining blisks with traditional point or flank milling. Cutting process will be deteriorated by cutter deflection and vibration and even be interrupted by cutter break-off. Plunge milling has been adopted widely to remove massive material in rough machining pockets, dies, and mold cavities [2]. Compared with the point and flank milling, the plunge milling has a larger axial but lower radial cutting force. Cutting conditions are improved in plunge milling, thanks to a higher rigidity of cutting tools in axial direction. To achieve a higher cutting efficiency and machining stability, the plunge milling is applied to machine open blisks in this paper.

When planning cutting tool paths, collision and interference between cutters and blisks must be avoided. Many effective approaches have been proposed and conducted to detect collisions and correct interferences. The configuration space (C-Space) method is widely used to obtain noninterference tool locations and orientation [3]. Morishige et al. [4, 5] projected obstacles onto a two-dimensional C-Space to get collision-free tool orientation in machining an impeller. The obstacles were divided into a set of triangular polygons and tool postures were represented by points on the boundaries of collision areas. Jun et al. [6] developed a boundary search method to find feasible tool orientation in the C-Space based on the edge detection technique. Suh and Lee [7] proposed a search algorithm to determine noninterference region of tool orientation in four-axis machining of free surfaces. This region is defined with two critical directions by updating and switching search direction based on discrete points. Although these are some effective ways to detect all possible tool orientation, quality and accuracy of calculated noninterference region are largely dependent upon the count of sampling points. Wu et al. [8] proposed an approach to generate noninterference tool path when machining impeller with a four-axis machine tool. The collision and interference were corrected by rotating tool axis vector timely. Considering local gouging and global interference, Chen and Liu [9] established a mathematical model of allowable cutter size and rotary table angle for each cutter contact (CC) point in four-axis machining to calculate the biggest allowable cutter and optimal tool orientation. Li et al. [10] presented a constrained optimization method to derive optimal tool orientation from feasible region for each CC point in five-axis machining of open blisks. These researches calculated tool orientation along a trajectory on the machined surface in point or flank milling. They selected plenty of points from tool trajectory as CC points and calculated tool orientation at them. In comparison, the plunger feeds along the tool axial direction and contacts the blade at only one or more than one CC point on one plunger path. It is time-consuming and redundant to calculate tool orientation at all points along the trajectory, because most of them are not CC points. Tool orientation in plunge milling needs to be determined first, and then the CC point(s) can be calculated with this determined tool orientation.

In four-axis plunge milling, the plunger rotates on a plane perpendicular to the blisk central axis. An intersection curve can be generated by intersecting this plane with the blade or offset surface of the blade. Some research has been conducted to seek plunger path from such an intersection curve. Ren et al. [11] and Shan et al. [12] adopted a series of straight lines to represent plunger paths when plunging an open blisk. A minimum area criterion was proposed and applied to calculate each straight line from intersection curve. This criterion is the area surrounded by the straight line and the intersection curve should be minimal on the plane. Li et al. [13] generated the straight line from intersection curve with the least-square method. This work aims at seeking a uniformly distributed machining allowance. Ren et al. [14] conducted another research on tool path planning in five-axis plunge milling of closed blisks. The intersection curves on offset surfaces of both hub and blade were taken into consideration to calculate the summing surrounded areas at each step. The researches mentioned above determined straight lines to approach intersection curves and then used them as the center axis of the plunger to cut the blade. Geometrically, owing to twisted structure of the blade, plungers on tool locations determined with this method may have overcut with the blade if no roughing allowance is applied. This method has been proved to be effective and acceptable in industry when offset value is equal to tool radius plus roughing allowance. However, the required roughing allowance cannot be guaranteed. Furthermore, this method only concerns about the relationship between intersection curve and straight line on a plane. The three-dimensional relationship of plunger and blade are not considered, which will be more accurate and reliable.

Compared with the blisk hub with high rigidity, slight cutting tools and thin-walled blades are prone to deflect and vibrate in the following point or flank milling. To reduce cutting forces, plunger paths are required to be planned appropriately to make sure that the residual material on the blade is as less as possible. To address this problem, a new approach is proposed in this paper to calculate noninterference plunger paths. In Section 2, the strategy to optimize tool orientation and calculate tool location is introduced. In Section 3, noninterference tool location in a given tool orientation is determined based on two principles established in Section 2. In Section 4, an evaluation criterion is proposed and applied to optimize tool orientation. In Section 5, a practical example is provided to demonstrate validity and advantages of this approach; and the work is concluded in Section 6.

2 Determination strategy of plunger paths

Figure 1 shows typical structure of an open blisk. Before rough milling, the blade portion of a blisk blank is machined on a lathe according to the profiles of leading and trailing edges of the blade. The geometric model of a blisk in this paper is prepared and modified as follows. First, offset suction and pressure surfaces along the outward normal direction of the blade with a given roughing allowance. Second, enlarge these offset surfaces and trim them by leading and trailing surface. Here, leading and trailing surface are surfaces of revolution on a blisk blank formed by a leading

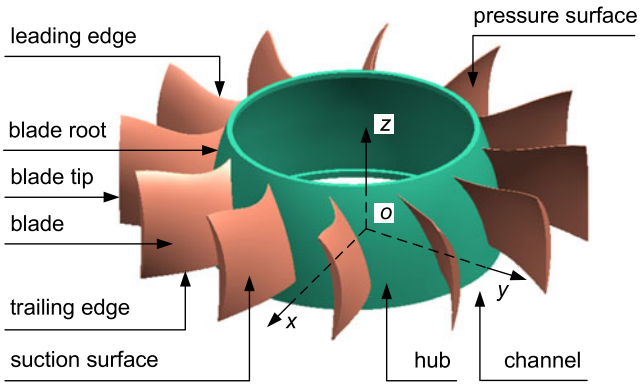

Fig. 1 Typical structure of an open blisk

and trailing edge, respectively. Third, trim enlarged surfaces near the blade root by the offset surface of the hub. A new channel can be formed by the offset surface of the hub and trimmed suction and pressure surfaces. When planning plunger paths in this new channel, roughing allowance is no longer a factor to be taken into consideration. For convenience, "new channel," "offset surface of hub," "trimmed suction surface," and "trimmed pressure surface" are called "channel," "hub," "suction surface," and "pressure surface," respectively, in the following part of this section and in the whole part of Section 3 and 4, unless otherwise specified.

Plunger paths to machine a channel can be classified into two types: boundary paths and internal paths. Boundary paths are a series of tool paths near the blades. They cut the blades and form their final shapes. The rest in this channel is called internal paths. They do not cut blades and have no impact on final shape of blades. The residual material on the blade affects the cutting load and cutting forces directly in semi-finishing and finishing processes. It evaluates the approaching extent of boundary paths to the blade. The main work in this paper is to determine boundary paths according to residual stock material on the blade.

In four-axis plunge milling, the plunger moves to a given position with a specified tool orientation and then removes material by feeding along the tool axis. To determine a plunger path, tool location and orientation in three-dimensional space need to be calculated. Compared with massive calculation in sample point method, a novel approach is proposed to calculate tool paths fast with projection contours of objects. In this method, tool orientation is determined first, and then tool location is calculated with this determined tool orientation. The "nearest" location of boundary path to the blade can be determined uniquely in a given tool orientation on the basis of two determination principles. They are noninterference principle and contact principle, respectively. The noninterference principle is that the cutter should not interfere with the hub, the currently machined blade, and the adjacent blade in the same channel. The interferences with tool shank, machine tools, and fixture are not discussed in this paper. The contact principle is that the cutter must contact the hub or the machined blade in tool axis direction and contact projection counters of the machined blade on a plane perpendicular to tool axis. A separate or untouched situation is not allowed. Based on these two determination principles, boundary tool locations can be uniquely determined according to tool orientation. This determination process will be introduced in detail in Section 3. When tool location and orientation are calculated, volume of residual material is also uniquely determined. The determination principles build a bridge to connect tool orientation and residual material together. Thus, this optimization problem evolves into seeking an optimal tool orientation for each tool path.

For instance, the suction surface of a blade is used as "machined surface" in the following part, while the pressure surface of adjacent blade in the same channel is called "adjacent surface".

3 Tool location calculation in a given tool orientation

To calculate tool location of the plunger in a given tool orientation, two coordinate systems are introduced. Denote the workpiece coordinate system shown in Fig. 1 as xyz coordinate system, in which z-axis is the central axis of the blisk and point o is the origin. Rotate the xyz coordinate system about the z-axis by angle θ and define it as rst coordinate system, as shown in Fig. 2. The origin of the rst coordinate system is also the point o. Here, angle θ represents tool posture in four-axis machining and r-axis is the tool orientation of one plunger path at the rotation angle θ. Tool location in a given tool orientation in four-axis plunge milling will be calculated as follows. First, calculate the projection contours of the blade and cutter on the sot plane (a plane passes through origin point t o, s-axis, and t-axis of the rst coordinate system). Then calculate the location of the projection contour of the cutter on the sot plane according to the determination principles mentioned above. Finally, calculate the r value of the cutter based on the determination principles in the rst coordinate system. Here, the r value denotes the maximum

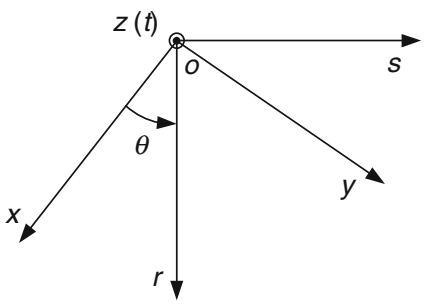

Fig. 2 Definition of the *rst* coordinate system

depth that the plunger can reach when feeding into the channel.

3.1 Projection contours of objects

A plunger or a flat-end mill is usually adopted as the cutter in plunge milling. Because of the axial-feeding pattern, the cutter can machine a cylindrical hole on the workpiece. In this paper, a cylinder is used to represent the cutter regardless of its exact shape. The contour of cutter on the *sot* plane is a circle, called cutter circle, as shown in Fig. 3. Its radius is equal to the radius of the cylinder, denoted as R_{tool}. It is worth to point out that the coordinate system shown in Fig. 3 just demonstrates directions of r-, s-, and t-axis, in which the origin of coordinate system is not specified. The same usage is applied in the following figures.

Geometrically, the projection of the blade surface on the *sot* plane contains two types of curve. One is the projection curves of surface boundaries, shown as curve C_1–C_4 in Fig. 3. The other is the projection curve of surface profile, shown as curve C_{P} in Fig. 3. The surface profile is a curve (curves) on the surface to divide the surface into visible and invisible parts when viewing the surface along negative r-axis direction.

Objects in the xyz coordinate system can be transformed onto the *sot* plane of the *rst* coordinate system by mapping and projecting. This transformation matrix $\mathbf{M}_{\text{MP}}(\theta)$ is

$$\mathbf{M}_{\text{MP}}(\theta) = \begin{bmatrix} 0 & 0 & 0 \\ -\sin\theta & \cos\theta & 0 \\ 0 & 0 & 1 \end{bmatrix} \tag{1}$$

Suppose the machined surface is $\mathbf{S}(u, v) = [S_x(u, v)\ S_y(u, v) S_z(u, v)]^{\text{T}}$. Four boundaries of this surface are $\mathbf{S}(u, 0)$, $\mathbf{S}(u, 1)$, $\mathbf{S}(0, v)$, and $\mathbf{S}(1, v)$. Uniformly, use the symbol n_i to represent the parameter of the ith surface boundary and denote the expression of boundaries in the xyz coordinate system as $\mathbf{S}_{\text{B}}(n_i) = [S_{\text{B},x}(n_i)\ S_{\text{B},y}(n_i)\ S_{\text{B},z}(n_i)]^{\text{T}}$ $(i = 1, 2, 3, 4)$. So, projection curves of boundaries on the *sot* plane, shown as curve C_1–C_4 in Fig. 3, can be expressed as follows:

$$\mathbf{C}_{\text{B}}(n_i, \theta) = \mathbf{M}_{\text{MP}}(\theta) \cdot \mathbf{S}_{\text{B}}(n_i) = \begin{bmatrix} 0 \\ -S_{\text{B},x}(n_i) \cdot \sin\theta + S_{\text{B},y}(n_i) \cdot \cos\theta \\ S_{\text{B},z}(n_i) \end{bmatrix} \tag{2}$$

In the xyz coordinate system, the view direction (negative r-axis) can be expressed as $\mathbf{V}(\theta) = [-\cos\theta \quad -\sin\theta \quad 0]^{\text{T}}$. The unit normal vector of the blade surface is

$$\mathbf{N}(u, v) = \begin{bmatrix} N_x(u, v) \\ N_y(u, v) \\ N_z(u, v) \end{bmatrix} = \frac{\frac{\partial S(u, v)}{\partial u} \times \frac{\partial S(u, v)}{\partial v}}{\left| \frac{\partial S(u, v)}{\partial u} \times \frac{\partial S(u, v)}{\partial v} \right|}$$

or

$$\mathbf{N}(u, v) = \begin{bmatrix} N_x(u, v) \\ N_y(u, v) \\ N_z(u, v) \end{bmatrix} = \frac{\frac{\partial S(u, v)}{\partial v} \times \frac{\partial S(u, v)}{\partial u}}{\left| \frac{\partial S(u, v)}{\partial v} \times \frac{\partial S(u, v)}{\partial u} \right|} \tag{3}$$

So, the surface profile at the rotation angle θ satisfies Eq. 4.

$$N_x(u, v) \cdot \cos\theta + N_y(u, v) \cdot \sin\theta = 0 \tag{4}$$

Equation 4 establishes a relationship between parameter u and v on the surface profile at rotation angle θ. In other words, according to Eq. 4, the surface profile can be expressed as a function of rotation angle θ and another parameter (represented with symbol w here). Denote the surface profile in the xyz coordinate system as $\mathbf{S}_{\text{P}}(w, \theta) = [S_{\text{P},x}(w, \theta) \quad S_{\text{P},y}(w, \theta) S_{\text{P},z}(w, \theta)]^{\text{T}}$. So the projection curve of surface profile on the *sot* plane, shown as curve C_{P} in Fig. 3, can be expressed as follows:

$$\mathbf{C}_{\text{P}}(w, \theta) = \mathbf{M}_{\text{MP}}(\theta) \cdot \mathbf{S}_{\text{P}}(w, \theta) = \begin{bmatrix} 0 \\ -S_{\text{P},x}(w, \theta) \cdot \sin\theta + S_{\text{P},y}(w, \theta) \cdot \cos\theta \\ S_{\text{P},z}(w, \theta) \end{bmatrix} \tag{5}$$

Equations 2 and 5 provide methods to calculate the projection curves of boundaries and surface profile, respectively. The maximum boundaries of all projection curves on the *sot* plane are the contours of blade surface on the *sot* plane, as shown in Fig. 3. These contours are composed of the part of projection curves of surface boundaries and profiles. Some deviation between the contours and projection curves is set in this figure to show them clearly.

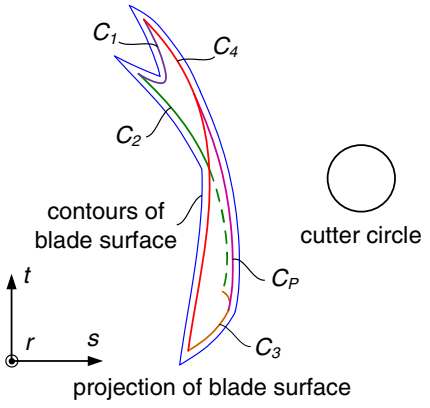

Fig. 3 Projections of cutter and blade surface on the *sot* plane

3.2 Location of the cutter circle on the *sot* plane

According to the determination principles, the cutter should be tangent to the machined surface. To achieve this objective, the calculation of tool location in three-dimensional

space can be converted into a two-dimensional plane (the *sot* plane) determined by a given tool orientation θ_g. This conversion reduces computation complexity. In four-axis plunge milling, plunger paths are determined on a series of axial heights of blisks. So tool location calculation and orientation optimization are all conducted when the axial height of the current tool is given. The cutter location is the center point O_c of the cutter circle on the *sot* plane, expressed by $[0 \quad s_{oc} \quad t_{oc}]^T$. On a given axial height t_g of the blisk, the cutter location is $[0 \quad s_{oc} \quad t_g]^T$. Then s_{oc} needs to be calculated to determine the location of cutter circle on the *sot* plane. The cutter circle may contact the blade contours on the *sot* plane in three potential situations: at projection points of surface vertexes, on projection curves of surface boundaries, and on projection curve of surface profile. So s_{oc} should be calculated in view of these three contacting situations.

1 At the projection points of surface vertexes. Suppose four vertexes of blade surface in the xyz coordinate system are $\mathbf{P}_{V,i} = [P_{V,i,x} \quad P_{V,i,y} \quad P_{V,i,z}]^T$ $(i = 1, 2, 3, 4)$. In this case, the distance from point O_c to the projections of vertexes should be equal to tool radius R_{tool} on the *sot* plane. s_{oc} can be calculated as follows:

$$s_{oc} = -P_{V,i,x} \cdot \sin\theta + P_{V,i,y} \cdot \cos\theta \pm \sqrt{R_{tool}^2 - (P_{V,i,z} - t_g)^2} \tag{6}$$

2 On the projection curves of surface boundaries. In this case, the cutter circle should be tangent to projection curve of one or more than one boundary. So the distance from point O_c to tangent point of curve C_1–C_4 should be equal to tool radius R_{tool}. And the vector determined by point O_c and tangent point should be perpendicular to the tangent vector of curve C_1–C_4 at the tangent point. On a given axial height t_g and at a given rotation angle θ_g, s_{oc} can be calculated with Eqs. 7 and 8 when two parameters (s_{oc} and n_i) are involved. Here, $S_{B,x}(n_i)'$, $S_{B,y}(n_i)'$ and $S_{B,z}(n_i)'$ are derivative of $S_{B,x}(n_i)$, $S_{B,y}(n_i)$ and $S_{B,z}(n_i)$ with respect to parameter n_i, respectively.

$$\left\| \begin{bmatrix} 0 \\ -S_{B,x}(n_i) \cdot \sin\theta_g + S_{B,y}(n_i) \cdot \cos\theta_g - s_{oc} \\ S_{B,z}(n_i) - t_g \end{bmatrix} \right\| = R_{tool} \tag{7}$$

$$\begin{bmatrix} 0 \\ -S_{B,x}(n_i) \cdot \sin\theta_g + S_{B,y}(n_i) \cdot \cos\theta_g - s_{oc} \\ S_{B,z}(n_i) - t_g \end{bmatrix}^T \cdot \begin{bmatrix} 0 \\ -S_{B,x}(n_i)' \cdot \sin\theta_g + S_{B,y}(n_i)' \cdot \cos\theta_g \\ S_{B,z}(n_i) \end{bmatrix} = 0 \tag{8}$$

3 On the projection curve of the surface profile. In this case, the cutter should be tangent to the profile of machined surface in three-dimensional space. The expression $\mathbf{C}_P(w, \theta)$ introduced in Eq. 5 is used to make description clear. However, the parameter w is hard to be obtained from Eq. 4. So in this case, tool location is calculated in three-dimensional space of the rst coordinate system. When the cutter contacts the profile curve of the blade surface at a contact point (points), we can find a point on the central line of the cutter which has the same r value with the contact point(s). Use this point as reference point to establish equations to calculate tool location. The distance from the contact point to the reference point should be equal to the tool radius R_{tool}. And the vector determined by the contact point and the reference point should be parallel to the normal vector of the blade surface at the contact point. These can be expressed as Eqs. 9 and 10 on a given axial height t_g and at a given rotation angle θ_g.

$$\left\| \begin{bmatrix} 0 \\ -S_x(u, v) \cdot \sin\theta_g + S_y(u, v) \cdot \cos\theta_g - s_{oc} \\ S_z(u, v) - t_g \end{bmatrix} \right\| = R_{tool} \tag{9}$$

$$\begin{bmatrix} 0 \\ -S_x(u, v) \cdot \sin\theta_g + S_y(u, v) \cdot \cos\theta_g - s_{oc} \\ S_z(u, v) - t_g \end{bmatrix} \times \begin{bmatrix} N_x(u, v) \cdot \cos\theta_g + N_y(u, v) \cdot \sin\theta_g \\ -N_x(u, v) \cdot \sin\theta_g + N_y(u, v) \cdot \cos\theta_g \\ N_z(u, v) \end{bmatrix} = 0 \tag{10}$$

In view of Eq. 4 at a given rotation angle θ_g, Eq. 10 can be written as follows:

$$\begin{bmatrix} 0 \\ -S_x(u, v) \cdot \sin\theta_g + S_y(u, v) \cdot \cos\theta_g - s_{oc} \\ S_z(u, v) - t_g \end{bmatrix}^T \cdot \begin{bmatrix} 0 \\ N_z(u, v) \cdot \cos\theta_g \\ -N_y(u, v) \end{bmatrix} = 0 \tag{11}$$

Then in this case, s_{oc} can be calculated by solving Eqs. 4, 9, and 11 with three parameters: u, v, and s_{oc}.

Following such a process, more than one cutter circle could be solved, as shown in Fig. 4. In this figure, circle C_{21} and C_{22}, circle C_{41} and C_{42}, and circle C_{P1} and C_{P2} are cutter circles solved by curve C_2, C_4, and C_P, respectively. A further judgment and selection is mandatory to get

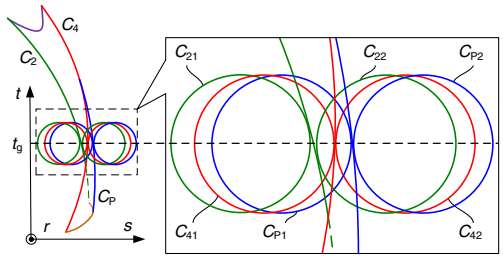

Fig. 4 Solved cutter circles on the *sot* plane

an expected noninterference cutter circle. This process is conducted as follows.

Step 1 Remove the cutter circles interfered with the projection contours of the machined surface on the *sot* plane. Calculate the minimum distance L_P from point O_c to curve C_P and the minimum distances $L_{B,i}$ $(i = 1, 2, 3, 4)$ from point O_c to curve C_1–C_4 in Fig. 3. If L_P or $L_{B,i}$ is less than R_{tool}, interference exists; then remove this point; otherwise, keep it.

Step 2 Remove the solved points located inside of the projection contours. Judge whether point O_c satisfies the expressions of s and t component of the surface $\mathbf{S}(u, v)$ in the rst coordinate system. If yes, remove this point; otherwise, keep it.

Step 3 Step 1 and step 2 are checking interference with the machined surface. Conduct step 1 and step 2 on the adjacent surface to remove the points interfered with adjacent surface in the current channel.

Step 4 Remove the points located completely outside of the current channel.

Following this judging process, there might be two situations. One is called absolute noninterference situation, as shown in Fig. 5. The region between the projection curves of the machined surface and the adjacent surface is called the machining region. For this situation, one expected noninterference solution can be obtained after the judging process. This solved point is used as the solved center point of the cutter circle on the *sot* plane.

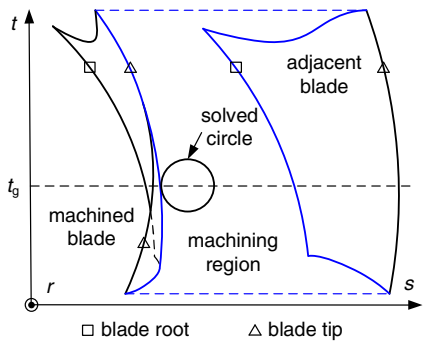

Fig. 5 Absolute noninterference situation to solve s value of the cutter

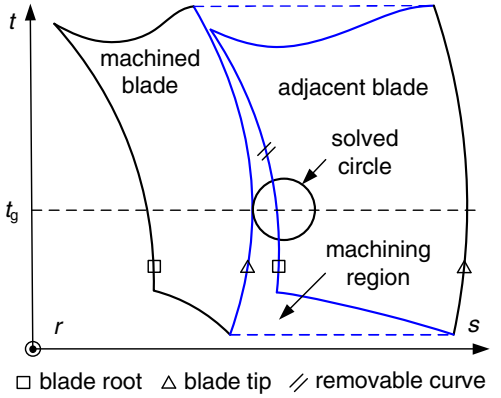

(a) Removable curve on the adjacent surface

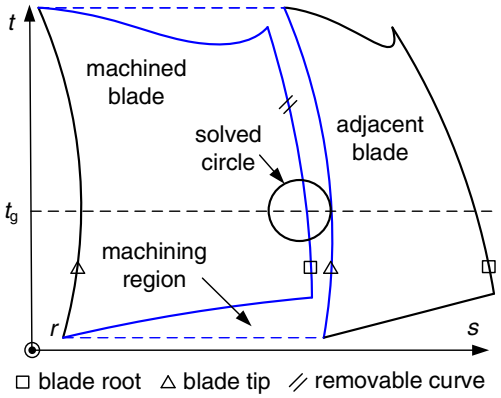

(b) Removable curve on the machined surface

Fig. 6 Conditional noninterference situation to solve s value of the cutter

And the other is called conditional noninterference situation, as shown in Fig. 6. Denote the projection curve of the blade root which forms the machining region as "removable curve". In Fig. 6a, the removable curve is the projection curve of the blade root of the adjacent surface. In Fig. 6b, it is the one of the machined surface. This situation is unusual if the cutter size and rotation angle are well selected. However, in this situation, no suitable solution can be obtained because the machining region is too narrow to get a noninterference circle on a given axial height t_g. To deal with it, the interference checking with the removable curve is skipped in Fig. 6a to get a conditional noninterference circle. In Fig. 6b, calculate the cutter circles from the adjacent blade. A conditional noninterference circle can be solved by skipping interference checking with the removable curve of the machined blade.

3.3 Cutting depth of the tool path

When the cutter circle is solved as an absolute noninterference solution shown in Fig. 5, the cutter can plunge into the

channel until contacting the hub. In this situation, the cutting depth is only decided by the hub surface, which is a surface of revolution. Suppose its generatrix curve on tor plane (a plane passes through origin point o, t-axis, and r-axis of the rst coordinate system) can be expressed as $t_h(m)$ and $R_h(m)$ for t and r coordinates. When the cutter, which is a cylinder, contacts the hub surface without interference, there should be two tangent situations as follows.

1 When $|s_{oc}|$ is less than R_{tool}, the hub surface is tangent to the base surface of the cylinder, in which the CC point is located on the inner portion of the base surface, as shown in Fig. 7a.
2 When $|s_{oc}|$ is no less than R_{tool}, the hub surface is tangent to the bottom edge of the cylinder, in which the CC point is located on the edge of the base surface, as shown in Fig. 7b.

In Fig. 7a, the cutting depth can be calculated as follows. The projection of the cutter cylinder on the tor plane is a rectangle, as shown in Fig. 8. The t values of the lower and upper profile of this cylinder are $t_g - R_{tool}$ and $t_g + R_{tool}$, respectively. The generatrix curve intersects the line $t = t_g - R_{tool}$ and $t = t_g + R_{tool}$ at point P_1 $(t_g - R_{tool}, r_1)$ and P_2 $(t_g + R_{tool}, r_2)$ on the tor plane. The maximum depth r_d that the cutter can reach in the channel along the current

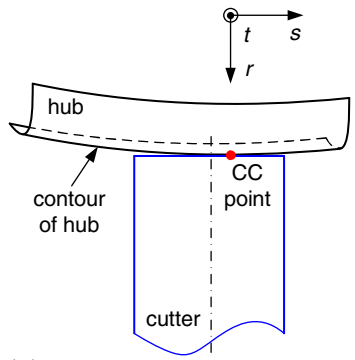

(a) CC point on the base surface of the cylinder

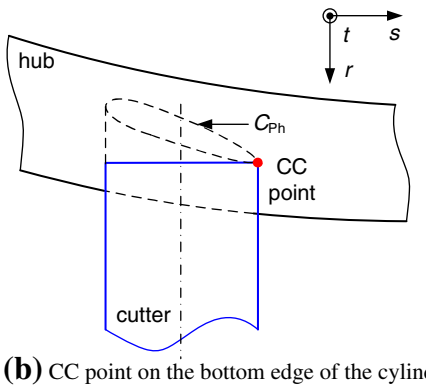

(b) CC point on the bottom edge of the cylinder

Fig. 7 Two tangent situations between the cutter cylinder and the hub surface

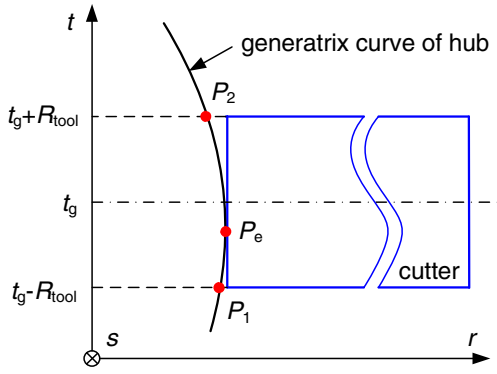

Fig. 8 Generatrix curve of hub on the tor plane

tool orientation is the maximum r value of the generatrix curve between points P_1 and P_2. Denote the parameter m of the generatrix curve at points P_1 and P_2 are m_1 and m_2, respectively. Then the maximum r value of the generatrix curve can be solved as $r_d = \max(r_1, r_2, r_e)$, in which r_e represents the maximum of all extreme r values on the generatrix curve in (m_1, m_2). It can be solved as $r_e = \max\left(R_h(m) \mid_{\frac{d(R_h(m))}{dm}=0}\right)$. If interval $[m_1, m_2]$ is not completely within the definition interval of the parameter m, the boundary points of the definition interval are required to be taken into consideration as well.

For the situation shown in Fig. 7b, the cutting depth can be calculated as follows. Denote the coordinates of CC point on the edge of the base surface as $[r_{cc} \quad s_{cc} \quad t_{cc}]^T$ in the rst coordinate system. The CC point is located both on the hub surface and the bottom edge of the cylinder, which can be expressed as follows:

$$r_{cc}^2 + s_{cc}^2 = {R_h}^2(m) \tag{12}$$

$$(s_{cc} - s_{oc})^2 + (t_{cc} - t_g)^2 = R_{tool}^2 \tag{13}$$

Substitute $t_{cc} = t_h(m)$ into Eq. 13 and combine it with Eq. 12. Then r_{cc} can be expressed as follows:

$$r_{cc}^2 = R_h^2(m) - (s_{oc} \pm \sqrt{R_{tool}^2 - (t_h(m) - t_g)^2})^2 \tag{14}$$

As shown in Eq. 14, r_{cc} is a function of parameter m. So it can be written as $r_{cc}(m)$. It represents the projection curve of the cutter on the hub surface along the negative r-axis, shown as curve C_{Ph} in Fig. 7b. The maximum depth r_d that the cutter can reach in the channel is equal to the maximum r value of the curve C_{Ph}, expressed as $r_d = \max(r_1, r_2, r_e)$. Here, $r_e = \max\left(r_{cc}(m) \mid_{\frac{d(r_{cc}(m))}{dm}=0}\right)$. r_1 and r_2 are the parameters at boundary points of curve C_{Ph} when a portion of curve C_{Ph} is outside of the hub surface.

When the cutter circle is solved as a conditional noninterference solution, as shown in Fig. 6, the blade surface associated with the removable curve needs to be considered to calculate the cutting depth. The CC point might be located on a curve projected by the cutter on this blade

surface along the negative r-axis. Similar calculation could be conducted as mentioned above.

4 Tool orientation optimization

4.1 Evaluation criterion for tool orientation

A new criterion is established in this section to evaluate tool orientation. This criterion is the following: the optimal tool orientation should be one which makes the cutter nearest to the machined blade on one plunger path determined by this tool orientation. In other words, the residual material on the machined blade determined by optimal tool orientation for one plunger path should be minimal. When calculating residual material for one tool path, previous tool paths have removed a part of the material and left an irregular shape on the blank. So the impacts of previous tool paths must be taken into consideration to present an in-process model of blank. In this case, the real residual material of the current boundary paths is the stock material between the current tool and the machined blade excluding the material removed by the previous tool paths.

A cutter on a given axial height t_g can only influence the stock material between plane $t = t_g - R_{tool}$ and $t = t_g + R_{tool}$ in the rst coordinate system. Entitle these two planes as the upper influence surface and the lower influence surface. Due to the specific shape of the blade leading and trailing edge, one of the influence surfaces may partly or completely be outside of the blisk blank for one plunger path. Usually, the upper influence surface of the first tool would be outside of the leading surface, while the lower influence surface of the last tool would be outside of the trailing surface. When defining residual material in this situation, the influence of leading and trailing surfaces needs to be taken into consideration.

Residual material is defined in Fig. 9. To demonstrate it clearly, the cutter in this figure does not contact the machined surface here, which is against the contact principle. The tool on the first axial height of the blisk is shown in Fig. 9a. In this case, the leading surface and the lower influence surface determine residual material in axial direction. Because a blisk is mainly a body of revolution and the cutter only contacts the hub or blade at a CC point, an influence surface of the cutter end is defined to determine the residual material in the cutting depth direction. The influence surface of the cutter end is a surface of revolution which is formed by revolving the inner part of the bottom edge of the cutter around the central axis of the blisk. So the residual material on this axial height is the material surrounded by the following six surfaces: machined surface, lateral surface of cutter, leading surface, lower influence surface, influence surface of the cutter end, and revolution surface of the blade tip.

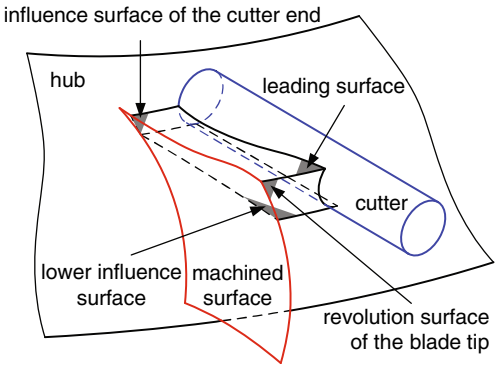

(a) Considering the leading surface

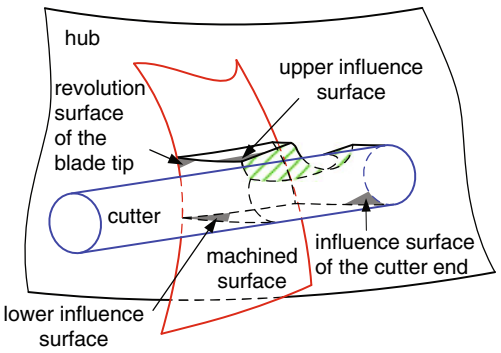

(b) Considering previous tool path(s)

Fig. 9 The definition of residual material

From the second tool path, residual material on each axial height should take the impacts of previous tool paths into consideration. A spatial region can be surrounded by the following six surfaces: machined surface, lateral surface of cutter, upper influence surface, lower influence surface, influence surface of the cutter end, and revolution surface of the blade tip. The previous tool path(s) has (have) removed part of the material in this spatial region. When tool location and orientation changes on this height, the effective material removed by the previous tool paths changes accordingly. So in this case, residual material on this height should be the material surrounded by the above six surfaces and the lateral surface (sometimes including base surface) of previous tool cylinders, which is shown in Fig. 9b with a hatching line.

4.2 Calculation of the residual material volume

A specific and practical method is proposed in this section to calculate the volume of the residual material, which is alternative and improvable. When calculating residual material, the influence surface of the cutter end, the upper influence surface, and the lower influence surfaces decide a region on the machined surface. Generally, the parameters u and v on the boundaries of this region are irregular. It is hard to apply an integration method to calculate the volume of the

residual material because limits of integration vary along region boundaries. Here, the volume of the residual material is calculated with a discrete element method as follows.

Step 1 Divide the residual material into thin slices in the axial direction of the blisk. The height of each slice is Δh, as shown in Fig. 10.

Step 2 Owing to the impacts of previous tool paths, slices on each height may be more than one piece. Divide each slice into elements in the radial direction with a radial height of ΔR, as shown in Fig. 10.

Step 3 When Δh and ΔR are small enough, each element can be treated as a body of revolution. Calculate the θ value of all the vertex points on this body in the rst coordinate system. Then, the element volume V_e can be calculated according to Eq. 15. Here, $\Delta\theta = \theta_{end} - \theta_{start}$. In Fig. 11, the mean value of angle θ of point P_{s1}, P_{s2}, P_{s3}, and P_{s4} is used as θ_{start}, while the mean value of angle θ of point P_{e1}, P_{e2}, P_{e3}, and P_{e4} is used as θ_{end}. $R_{inner} = (R_1 + R_2)/2$ and $R_{outer} = (R_3 + R_4)/2$. R_1, R_2, R_3, and R_4 are radius of the four edges on the element.

Step 4 Add the volume of all elements together as the volume of residual material for each tool path.

$$V_e = \frac{1}{2}(R_{outer}^2 - R_{inner}^2)\Delta\theta\,\Delta h \tag{15}$$

4.3 Tool orientation optimization process

Owing to the irregular shape of the residual material and undecided cutter contact point for the tool path in advance,

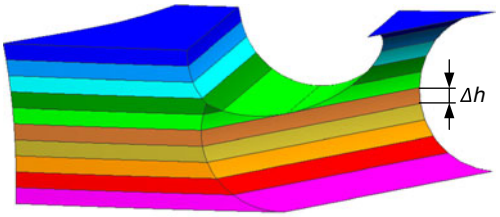

(a) Dividing into slices

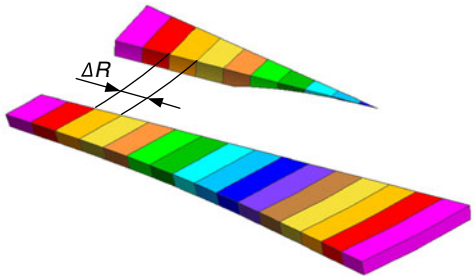

(b) Dividing into elements

Fig. 10 Division of residual material

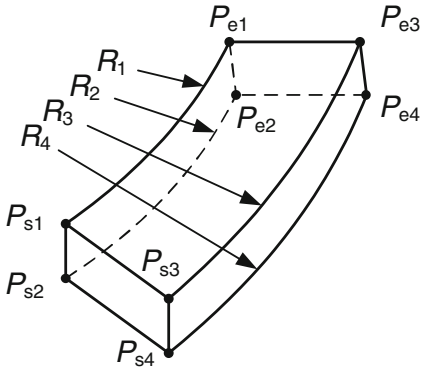

Fig. 11 Calculation of element volume

tool orientation optimization in this paper is a global non-differentiable optimization problem. The particle swarm optimization (PSO) method is employed and conducted to address this problem. In PSO method, rotation angle θ and volume of residual material are used as particle position and fitness value, respectively. This process is conducted as follows.

Step 1 Specify a series of axial heights for a blisk.

Step 2 Set a rotation interval for angle θ on a given axial height of the blisk. Suppose that the lower and upper limits of this interval are angle θ_1 and θ_2, respectively. They can be calculated approximately as follows. Denote the blade root and tip of the machined surface as edge E_{mr} and E_{mt}, respectively, while those of the adjacent surface are edge E_{ar} and E_{at}. In an rst coordinate system decided by angle θ_1, express s value of edge E_{ar} and E_{mt} as $s_{ar}(\theta_1)$ and $s_{mt}(\theta_1)$, respectively. Then, solve the angle θ_1 from Eq. 16. In an rst coordinate system decided by angle θ_2, express s value of edge E_{at} and E_{mr} as $s_{at}(\theta_2)$ and $s_{mr}(\theta_2)$, respectively. Solve the angle θ_2 from Eq. 17. When the tool orientation is near the angle θ_1 or θ_2, the inclination angle between the cutter and machined surface is very great to result in a large volume of residual material. The final optimal tool orientation will be far away from these two limit angles. So, such a calculation for the lower and upper limits is good enough to set a rotation interval for angle θ.

$$s_{ar}(\theta_1) - s_{mt}(\theta_1) = 2R_{tool} \tag{16}$$

$$s_{at}(\theta_2) - s_{mr}(\theta_2) = 2R_{tool} \tag{17}$$

Step 3 Initialize the speed and position for all particles on the rotation interval.

Step 4 Calculate the tool location in the current tool orientation with the method proposed in Section 3. Here, the current tool orientation is preset as the particle position.

Step 5 Calculate the volume of residual material on the current location and orientation.

Step 6 Use the volume of residual material as the fitness value and seek the tool orientation with the minimum residual material with PSO method.

Step 7 Conduct step 2 to step 6 until the tool orientation on each axial height has been optimized.

5 Applications

5.1 Tool path generation

To demonstrate its advantages in optimizing noninterference tool path, this approach is applied to machine an open blisk shown in Fig. 1 based on a modified PSO method. There

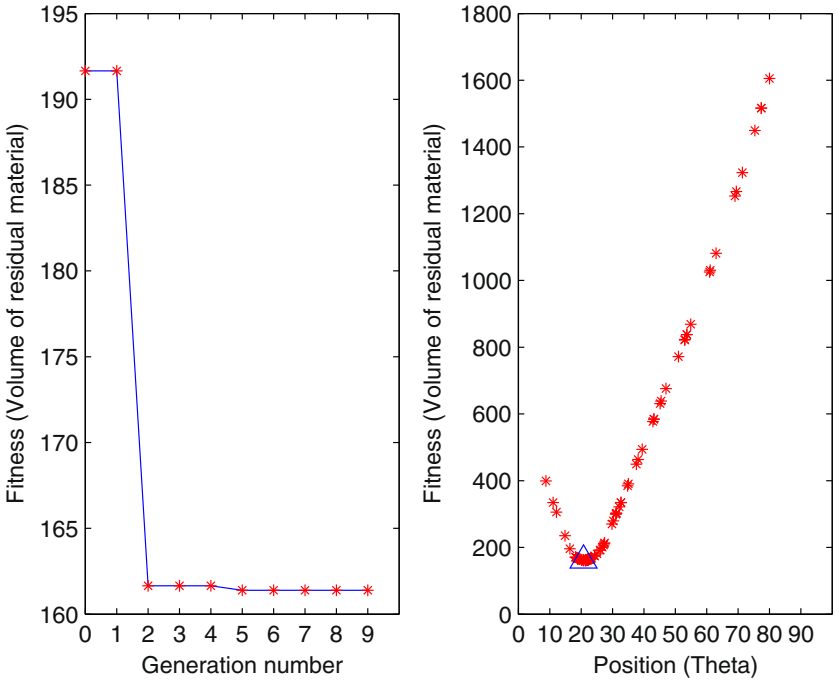

(a) Suction surface

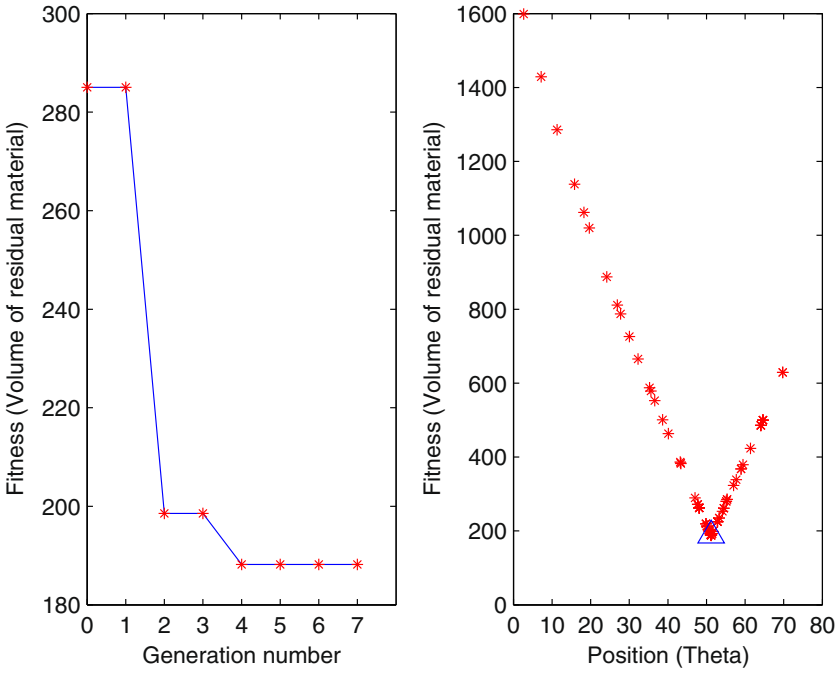

(b) Pressure surface

Fig. 12 Optimization processes on one axial height

are 12 blades on this open blisk. The angle between two blades is 30°. The forging blank of this blisk is a titanium alloy (Ti-6Al-4V) cylinder with height of 45 mm and diameter of 177 mm. A flat-end mill with a diameter of 10 mm is adopted. Tool paths have been divided into seven layers in axial direction with axial height of 6.5 mm. Machining allowance for plunge milling is set to be 0.75 mm. PSO parameters are set as follows. Population size of particles is set to be ten. The inertia weight is decreased linearly from 0.9 to 0.4 to provide a balance between global and local search based on an empirical study conducted by Shi and Eberhart [15]. Time-varying acceleration coefficients are used to change two acceleration coefficients from 2.5 to 0.5 and from 0.5 to 2.5, respectively, based on the research in reference [16]. The maximum velocity is decreased linearly from 10 % of rotation interval at the beginning to 1 % at the end. The PSO process will terminate when rotation angles of all particles move within a tolerance of 10^{-3} degrees or the generation number reaches at 30.

Tool path calculation proposed in this paper have been implemented in MATLAB R2011b. The optimization processes for suction and pressure surface of the blade on one axial height are shown in Fig. 12. The left part of each subfigure shows the relationship between the generation number and the best fitness that all particles can get until this generation. The right part of each subfigure shows the relationship between the particle position and fitness, which means the relationship between tool orientation, represented with rotation angle θ, and corresponding volume of residual material. The triangle shows the optimized tool orientation on the current axial height. By repeating this approach, all optimized boundary paths in one channel can be obtained in MATLAB, as shown in Fig. 13.

When boundary paths on the suction surface and pressure surface have been optimized, internal paths are interpolated between them with a constant rotation angle, which varies

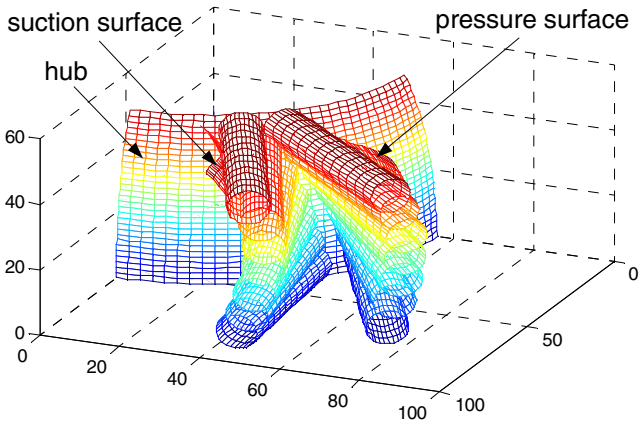

Fig. 13 Optimized boundary paths

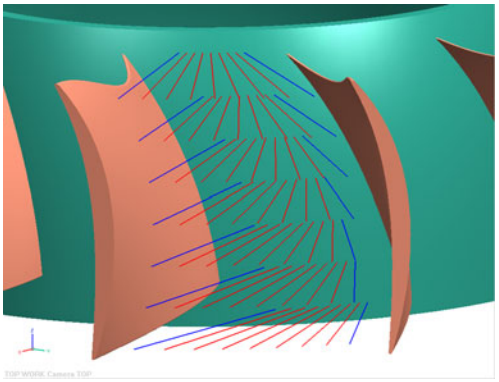

Fig. 14 Boundary and internal paths for one channel

among different axial heights. Cutting depths of interpolated tool paths are calculated with the method described in Section 3. Boundary and internal paths are demonstrated in Fig. 14 with central lines of cutters in Siemens NX 7.0. The blisk is machined with a carbide flat end mill in MAHO 60E machining center to verify the approach proposed in this paper, as shown in Fig. 15.

5.2 Comparison and analysis

The main objective of this work is to generate noninterference plunger paths to reduce residual material on machined surfaces. Relevant work can be discovered in reference

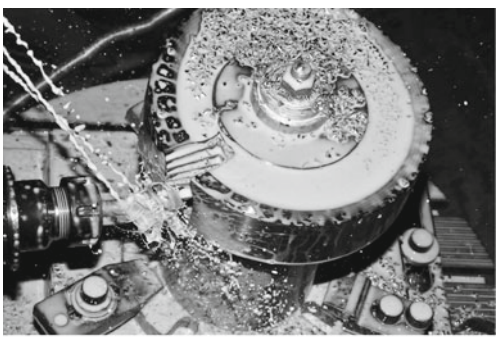

(a) Machining process

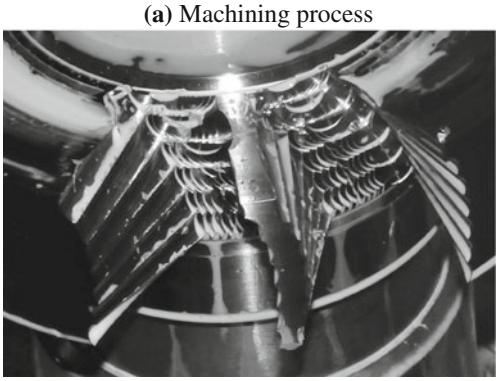

(b) Machined channels of blisk

Fig. 15 Plunge milling experiment

[11–13] in literature review. Reference [13] aims at getting a uniformly distributed machining allowance. It will leave more residual material on machined blade than the approaches proposed by reference [11] and [12], which have a similar result. This paper is an extension of the previous research in reference [11]. To compare them, the same blisk, cutter, cutting parameters, and machining allowance are used to optimize tool orientation of boundary paths. Comparison and analysis are shown as follows.

When ignoring machining allowance, boundary paths generated in this paper have no interference both with the blades and hub. Boundary paths obtained by the previous method have no interference with suction surface of the blade and hub. But interferences can be detected on the pressure surface of the blade. In practical production, machining allowance must be reserved for the following semi-finishing and finishing processes. When setting the machining allowance as 0.75 mm, the minimum distances between the blade and boundary paths are all equal to the machining allowance in this paper. Thanks to the machining allowance, interferences that occurred with previous method are eliminated. But the required machining allowance cannot be guaranteed on two tool paths. In experiment, minimum distances between the blade and these tools are 0.698 and 0.747 mm, respectively.

The total volume of residual material on suction surface on plunger paths determined in this paper is 1,218.91 mm^3, which is 1,264.71 mm^3 with the previous method. The residual material on suction surface reduces by 3.62 % with the method proposed in this paper. It is mainly because this method calculates the volume of residual material in three-dimensional space and the impacts of previous tool paths have been considered. It is more accurate and practical. The total volume of the residual material on the pressure surface in this paper is 2,048.75 mm^3, which is 2,017.92 mm^3 with the previous method. Although the previous work has a 1.50 % lower residual material than this work, it is at the expense of unsatisfied machining allowance. It will affect the cutting conditions of the following semi-finishing and finishing processes, especially for blisks with thin and large blades. The unsatisfied parts of surface are critical when deciding boundary paths.

In the previous work, the failure to get the expected plunger paths is mainly because plunger paths are determined by straight lines derived from intersection curves on planes. Generally, the pressure surface of blade is a twisted concave surface, while the suction surface is convex. A cylinder located on such a straight line may have overcut on the pressure surface with a certain curvature radius and twisted angle. When calculating the tool location with a cylinder in three-dimensional space with the proposed method, such an error can be eliminated. In summary, the approach proposed in this paper can guarantee the expected machining allowance and get "closer" noninterference tool paths than the previous work. It is more efficient and reliable by taking into account an in-process model of blank in three-dimensional space.

6 Conclusions

A novel approach to optimizing tool orientation and determining noninterference tool locations for four-axis plunge milling of open blisks has been proposed. The main contributions of this work include that (a) a novel approach to calculating noninterference tool locations with projection contours of objects, (b) a new evaluation criterion for optimizing the tool orientation considering spatial structure of the blade and impacts of previous tool paths, and (c) a practical method of calculating the volume of irregular residual material on the blade surface. In this approach, an in-process model of the blisk is adopted for higher accuracy. By applying a modified PSO method, tool orientation and corresponding noninterference locations are optimized to machine an open blisk. This approach has been proved to be efficient and reliable to plan tool paths for four-axis plunge milling. It can be used to machine similar types of blisks and impellers in industry.

Acknowledgments This work was supported by the National Science and Technology Major Project of China (no. 2013ZX04011031).

References

1. Younossi O, Arena MV, Moore RM, Lorell M, Mason J, Graser JC (2002) Military jet acquisition: technology basics and cost-estimating methodology. RAND, Santa Monica
2. Ko JH, Altintas Y (2007) Time domain model of plunge milling operation. Int J Mach Tools Manuf 47:1351–1361
3. Lasemi A, Xue DY, Gu PH (2010) Recent development in CNC machining of freeform surfaces: a state-of-the-art review. Comput-Aided Des 42(7):641–654
4. Morishige K, Kase K, Takeuchi Y (1997) Collision-free tool path generation using 2-dimensional C-space for 5-axis control machining. Int J Adv Manuf Technol 13:393–400
5. Morishige K, Takeuchi Y (1997) Five-axis control rough cutting of an impeller with efficiency and accuracy. Proc IEEE Int Conf Robot Autom 2:1241–1246
6. Jun CS, Cha K, Lee YS (2003) Optimizing tool orientations for 5-axis machining by configuration-space search method. Comput-Aided Des 35(6):549–566
7. Suh SH, Lee KS (1992) Avoiding tool interference in four-axis NC machining of rotationally free surfaces. IEEE Trans Robot Autom 8(6):718–729
8. Wu BH, Zhang DH, Luo M, Zhang Y (2013) Collision and interference correction for impeller machining with non-orthogonal four-axis machine tool. Int J Adv Manuf Technol 68:1–8
9. Chen ZC, Liu G (2007) Automated tool-orientation determinations for 4-axis non-gouge, non-interference milling of axial-flow

compressors airfoils. Proc ASME Turbo Expo Gas Turbine Tech Congr Expo 5:147–154
10. Li S, Tang M, Luo M (2011) Optimal tool orientation planning for five-axis machining of open blisk. Proc Fourth Int Conf Intell Comput Technol Autom 2:1138–1141
11. Ren JX, Yao CF, Zhang DH, Xue YL, Liang YS (2009) Research on tool path planning method of four-axis high-efficiency slot plunge milling for open blisk. Int J Adv Manuf Technol 45(1):101–109
12. Shan CW, Zhang DH, Ren JX, Hu CG (2006) Research on the plunge milling techniques for open blisks. Mater Sci Forum 532-533:193–196
13. Li T, Chen WY, Chen CH (2010) Rough machining method for blisk plunge milling. Comput Integr Manuf Syst 16(8):1696–1701
14. Ren JX, Xie ZF, Liang YS, Yao CF, Liu B (2010) 5-axis plunge milling path planning of closed blisk. Acta Aeronaut Astronaut Sin 31(1):210–216
15. Shi Y, Eberhart RC (1999) Empirical study of particle swarm optimization. Proc IEEE Int Congr Evol Comput 3:1945–1950
16. Ratnaweera A, Halgamuge SK, Watson HC (2004) Self-organizing hierarchical particle swarm optimizer with time-varying acceleration coefficients. IEEE Trans Evol Comput 8(3):240–255